ORIGINAL PAPER

Evaluation of fine material and chip formation in rock cutting with a conical tool

Mohammad Hossein Kadkhodaei[1] · Ebrahim Ghasemi[1] · Jafar Khademi Hamidi[2] · Jamal Rostami[3]

Abstract

The production of fines and chips during rock cutting plays an essential role in the efficiency of rock cutting, which in turn impacts productivity and performance of mechanical excavators. In this study, small scale linear rock cutting experiments were conducted using a conical tool on thirteen sedimentary and metamorphic rock samples to evaluate the transition between ductile to brittle cutting mode by examining the volume of fines versus chips produced in the process of cutting. Cuts with depths of 0.5, 0.8, 1, 2, 3, 4, 5, and 6 mm were made to investigate the production of fines and chips in unrelieved cutting mode. The forces acting on the conical tool, cutting rate, and volume of fines were measured. Initially, the critical cutting depth was determined by analyzing the cutting force signals, aiming to identify both ductile and brittle cutting failure zones. Subsequently, the percentage of fines were classified into three classes using the hierarchical clustering algorithm. Finally, the support vector machine algorithm was employed to create a two-dimensional space utilizing cutting parameters, enabling the identification of the fines to chip transition zone. The effective cutting depth was determined based on specific energy variations, and subsequently, the effective limit was determined in the fines transition zone. The results showed that cutting depths lower than the critical value lead to the production of high fines under ductile failure mode. Also, the results obtained from assessing the performance of the two-dimensional fines space, predicated on cutting parameters, demonstrated that the developed model effectively evaluates the fines transition zone with a high level of accuracy. The results of this study can help in managing the fines production.

Abbreviations

FM	Fine material	F_{Tmax}	Maximum resultant force
CH	Chip	F_{Tavg}	Average resultant force
UCS	Uniaxial compressive strength	d	Cutting depth
BTS	Brazilian tensile strength	ΔF	Cutting force difference
D	Density	ΔT	Cutting time difference
P	Porosity	Ra	Ratio of cutting force difference to cutting time difference
		SLR	Slope of the linear fit
		HC	Hierarchical clustering
		CR	Cutting rate
		SVM	Support vector machine
		SVC	Support vector classification
		OAO	One-against-one algorithm
		OAA	One-against-all algorithm
		SE	Sensitivity
		AC	Accuracy
		SP	Specificity
		MCC	Matthew's correlation coefficient

✉ Ebrahim Ghasemi
  e_ghasemi@iut.ac.ir

1. Department of Mining Engineering, Isfahan University of Technology, Isfahan 8415683111, Iran

2. Mining Engineering Department, Faculty of Engineering, Tarbiat Modares University, Jalal Ale Ahmad Highway, P.O. Box 14115-111, Tehran, Iran

3. Department of Mining Engineering, Earth Mechanics Institute (EMI), Colorado School of Mines, Golden, CO, USA

TP   True positive
FP   False positive
TN   True negative
FN   False negative
d_{Min} Minimum effective cutting depth

Introduction

In mechanical rock excavation, evaluation of fine material (FM) and chip (CH) production is an important aspect of the cutting process that affects the efficiency of operations. Generally, the rock failure mechanism depends on the cutting depth and the type of rock being cut, involving two modes: brittle and ductile. At smaller cutting depths (mainly when the cutting depth is less than 1 mm), the rock failure mechanism is ductile, but as the cutting depth increases, it shifts to the brittle mode (Rostamsowlat et al. 2022). Consequently, this change in the rock failure mechanism results in an increased ratio of CH production to FM production.

The cutting depth is often a limiting factor, due to the need for sufficient cutting forces, that in turn is limited by the cutter load capacity. Therefore, it is crucial to determine maximum cutting depth to ensure efficient excavation operations without compromising the overall performance and integrity of the cutting tools. Pick cutters (conical tools) are widely used for excavating rocks with weak to medium strength and in nonabrasive soft grounds such as salt, potash, and coal (Martin and Fowell 1997; Hood and Alehossein 2000; Bilgin et al. 2014). Due to the type of rock to be excavated and the machines that utilize this tool (roadheaders, shearer loaders, and continuous miners), the boundary between FM and CH production becomes more critical.

Figure 1 shows schematic of FM and CH during rock cutting with conical cutting tool. According to this figure, when the cutting tool hits the rock, FM is generated through the crushed zone and scratching on the rock at the micro scale, while CH is formed through the development of tensile cracks that extend to the surface of the rock.

If the cutting conditions required for the propagation of tensile fractures are not achieved, either due to the necessity for increased cutting depth or the machine's limited power, grinding will occur within the crushed zone. Grinding produces only fines instead of chips, resulting in a significantly reduced penetration rate. Chipping, on the other hand, represents a more efficient excavation process because the generation of chips through tensile fracturing is much more efficient than the formation of fines within the crushed zone (Snowdon et al. 1982; Gertsch et al. 2007). During the mechanized excavation operation, as other aspects of the operation such as cutting tool wear affect the efficiency of the operation (Wei et al. 2018, 2019, 2021, 2023; Elbaz et al. 2021), the greater the amount of FM, the lower the efficiency of cutting and the productivity of the excavation unit can be expected. Evaluation of FM and CH production affects the amount of production dust, ventilation costs, personnel health, tool wear, and cutting forces as mentioned
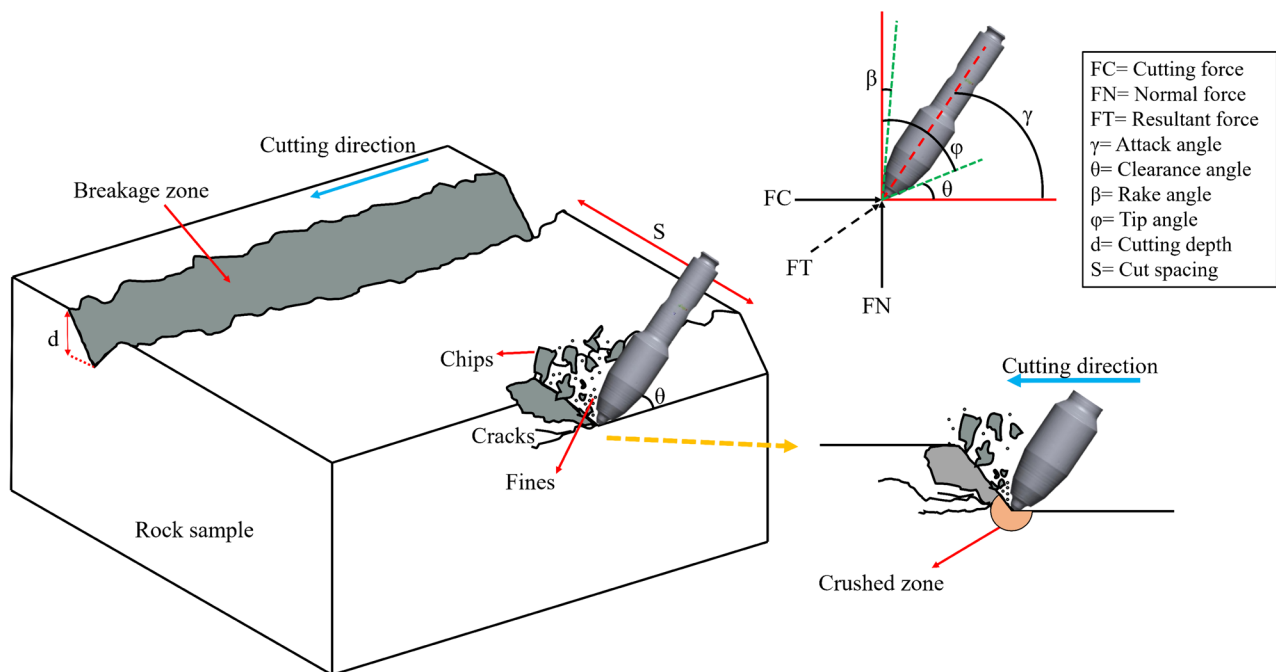
Fig. 1 Schematic of FM and CH during rock cutting with conical cutting tool

by Roxborough et al. (1981), Mohammadi et al. (2020), and Bejari and Hamidi (2023). Additionally, breaking a volume of rock into chips requires less energy than breaking it into fines (Vogt 2016).

In the field of mechanized excavation, extensive studies have been conducted on the production of FM and CH from rock cutting, as well as their characteristics and their impact on excavation performance (e.g. Barker 1964; Roxborough 1973; Roxborough et al. 1981; Ip 1986; Bruland 2000; Gertsch et al. 2000; Rostami et al. 2002, 2020; Altindag 2003, 2004; Gong et al. 2007; Tuncdemir et al. 2008; Balci 2009; Abu Bakar and Gertsch 2011; Yin et al. 2014; Abu Bakar et al. 2014; Rispoli et al. 2017; Jeong and Jeon 2018; Pan et al. 2018; Heydari et al. 2019; Mohammadi et al. 2020; Pourhashemi et al. 2021; Hou et al. 2021; Huang et al. 2022; Bejari and Hamidi 2023). The past studies on this topic have provided valuable insights into how the composition and quantity of FM and CH generated during the cutting process can influence the overall efficiency and effectiveness of excavation operations. The results of the past studies shows that, in general, the higher the amount of CH production, the better the excavation performance. In addition, according to Rostamsowlat et al. (2022), increase in cutting depth results in an increased ratio of CH to FM ratio due to entering the brittle cutting mode.

A quick review of the literature indicates that extensive studies have been conducted on the effect of CH and FM production, as well as the dimensions of the fragments resulting from cutting, on the cutting performance. However, a comprehensive investigation has not been presented to determine the limit of FM production and establish effective rock cutting conditions, mainly due to the limited size of data sets that researchers can access for such analysis. In this study, the boundary of FM production during rock cutting using the conical tool has been investigated. For this purpose, cutting with a conical tool at various depths was performed on thirteen weak to medium strength (based on Bieniawski (1989) classification) laboratory-scale rock samples. The cutting tests were followed by sieve analysis of the fragments collected from sample surface. The threshold penetration for transition from FM production to efficient chipping was investigated using the support vector machine algorithm.
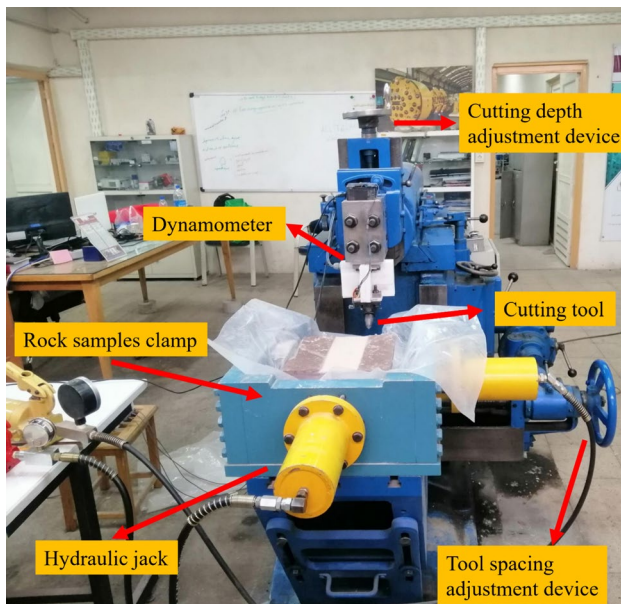
Laboratory testing

In this study, thirteen rock samples, comprising gypsum, salt, kaolin, travertine, and marble, were gathered from different locations in Iran with different geological settings. It includes sedimentary and metamorphic samples were collected from quarry/mine sites. Then the samples were prepared for rock mechanics tests and cutting operations. Rock mechanics tests, including uniaxial compressive strength (UCS), Brazilian tensile strength (BTS), density (D), and porosity (P), were conducted on each sample following the standards set by ASTM and ISRM (ASTM D2938-95 1995; ASTM D3967-95 1995; ASTM D4543-08 2008). Table 1 shows the physical and mechanical properties of rock samples. According to the table, the studied samples cover a wide range of rock types that can be cut with a conical tool, ranging from weak to medium, as per Bieniawski (1989) classification.

Cutting tests were carried out on each rock sample at various cutting depths of 0.5, 0.8, 1, 2, 3, 4, 5, and 6 mm using the small-scale linear cutting machine (SSLCM) at the Mechanized Excavation Laboratory of Tarbiat Modares University (MEL-TMU) as shown in Fig. 2. This machine has a power of 5.9 kW and a maximum cutting stroke of 90 cm. The position of the cutting stroke in the test rig can be modified based on the length of the rock sample in the cutting direction. In this study, a constant cutting speed of

Table 1 Physico-mechanical properties of the studied rocks

| Rock Sample	Commercial name	Sample code	UCS (MPa)	BTS (MPa)	D (g/cm^3)	P (%)
Sandstone	Ghermez-Qom	S1	59.19 ± 4.2	4.65 ± 0.27	2.23	6.64
Kaoline	Zanjan	S2	15.53 ± 0.9	1.32 ± 0.10	2.13	19.01
Salt rock	Semnan	S3	18.21 ± 0.9	1.8 ± 0.17	2.10	31.36
Gypsum	Ardestan	S4	11.08 ± 0.5	1.33 ± 0.09	2.25	16.39
Travertine	Targh	S5	65.89 ± 2.6	3.74 ± 0.21	2.34	5.91
Travertine	Dare-Bokhari	S6	66.40 ± 4.5	3.98 ± 0.33	2.48	7.36
Travertine	Asali	S7	56.49 ± 4.2	4.58 ± 0.22	2.47	7.8
Travertine	Limoei	S8	54.40 ± 3.7	3.21 ± 0.21	2.36	5.66
Travertine	Bookan	S9	44.86 ± 2.1	2.97 ± 0.39	1.97	14.86
Travertine	Abbas-Abad	S10	49.54 ± 3.2	5.00 ± 0.24	2.48	5.96
Travertine	Chocolate	S11	51.76 ± 2.3	5.41 ± 0.39	2.46	8.32
Travertine	Ghermez-Azarshahr	S12	53.71 ± 2.9	4.65 ± 0.27	2.25	6.94
Marble	Marvdasht	S13	92.36 ± 5.7	6.38 ± 0.17	2.56	3.96

Fig. 2 View of the small-scale linear cutting machine (SSLCM) at the Mechanized Excavation Laboratory of Tarbiat Modares University (MEL-TMU)

25 cm/s is considered for all tests. In addition, the conical cutting tool connected to the machine is designed based on the attack angle of 50 degrees and the clearance angle of 5 degrees. For each sample in unrelieved mode, the force acting on the conical tool (including cutting, normal, and side forces) were measured using a 3D load cell with a sampling frequency of 500 Hz. In a linear cutting operation, since the tool does not move sideways, forces only act on the conical tool in two directions: along the cutting direction and perpendicular to it. Therefore, the force acting on the cutting tool is equivalent to the combination of two forces: the cutting force and the normal force.

Figure 3 shows the resultant force signal of sample S1. After determining the resultant forces for rock cutting, the maximum resultant force (F_{Tmax}) and average resultant force (F_{Tavg}) are employed for analysis. It is important to note that F_{Tmax} is calculated as the average of the three peak values, while F_{Tavg} is the average of the resultant force for a given cutting test (sum of average of individual lines). Figure 4 shows the relationship between F_{Tmax}, F_{Tavg}, and cutting depth (d). According to the figure, there is a direct relationship between cutting depth, F_{Tmax}, and F_{Tavg}. The results of this study align with available literature (Evans and Pomeroy 1966; Nishimatsu 1972; Bilgin 1977; Bilgin et al. 2014; Morshedlou et al. 2023).

Additionally, the fragments collected from the cutting were carefully collected and subjected to sieve analysis. Based on Wentworth (1922) classification, the fragments were then classified into three categories: fine (particle
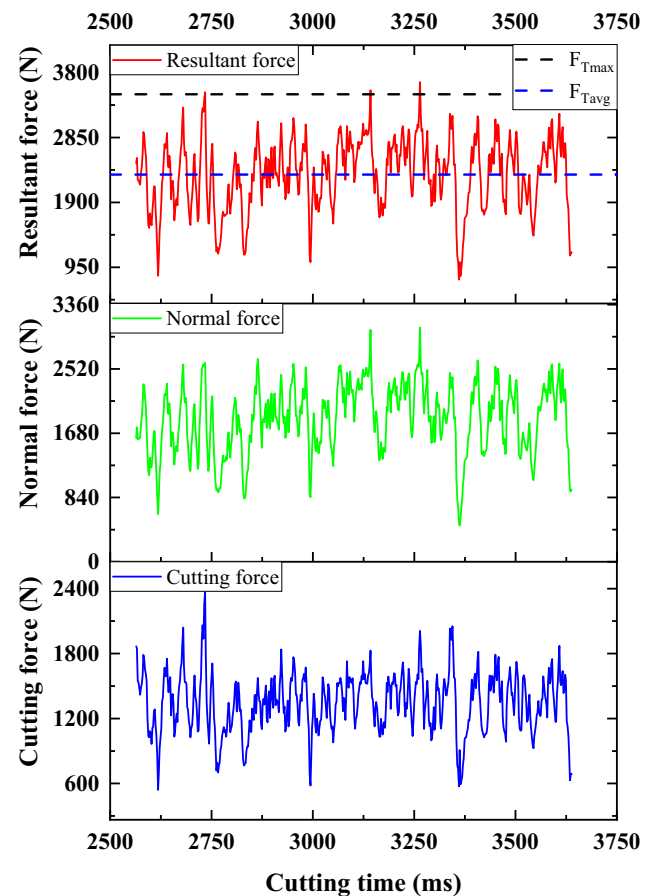
Fig. 3 The resultant force signal in time domain of S1 sample at cutting depth of 3 mm

diameter less than 1.2 mm), medium (particle diameter between 1.2 to 4.75 mm), and chip (particle diameter larger than 4.75 mm). Figure 5 shows the classification of fragments obtained from cutting the S9 rock sample. As seen, as the cutting depth increases, the amount of fines compared to the volume of fragments decreases, while the amount of chips increases. The findings of this study are consistent with those of previous research (Copur et al. 2003; Tuncdemir et al. 2008; Jeong and Jeon 2018; Dai et al. 2021; Wang et al. 2022).

Results and discussion

Critical cutting depth

As mentioned, when the depth of cut in the rock increases, the cutting mode tends to become more brittle, consequently leading to an increase in the CH to FM ratio. On the other hand, the cutting force is directly related to the interaction between the rock and the cutting tool. When the cutting tool starts its penetration into the rock, the cutting

Fig. 4 The relationship between the cutting depth and force features: **a)** F_{Tmax}-d and **b)** F_{Tavg}-d

(a)

(b)
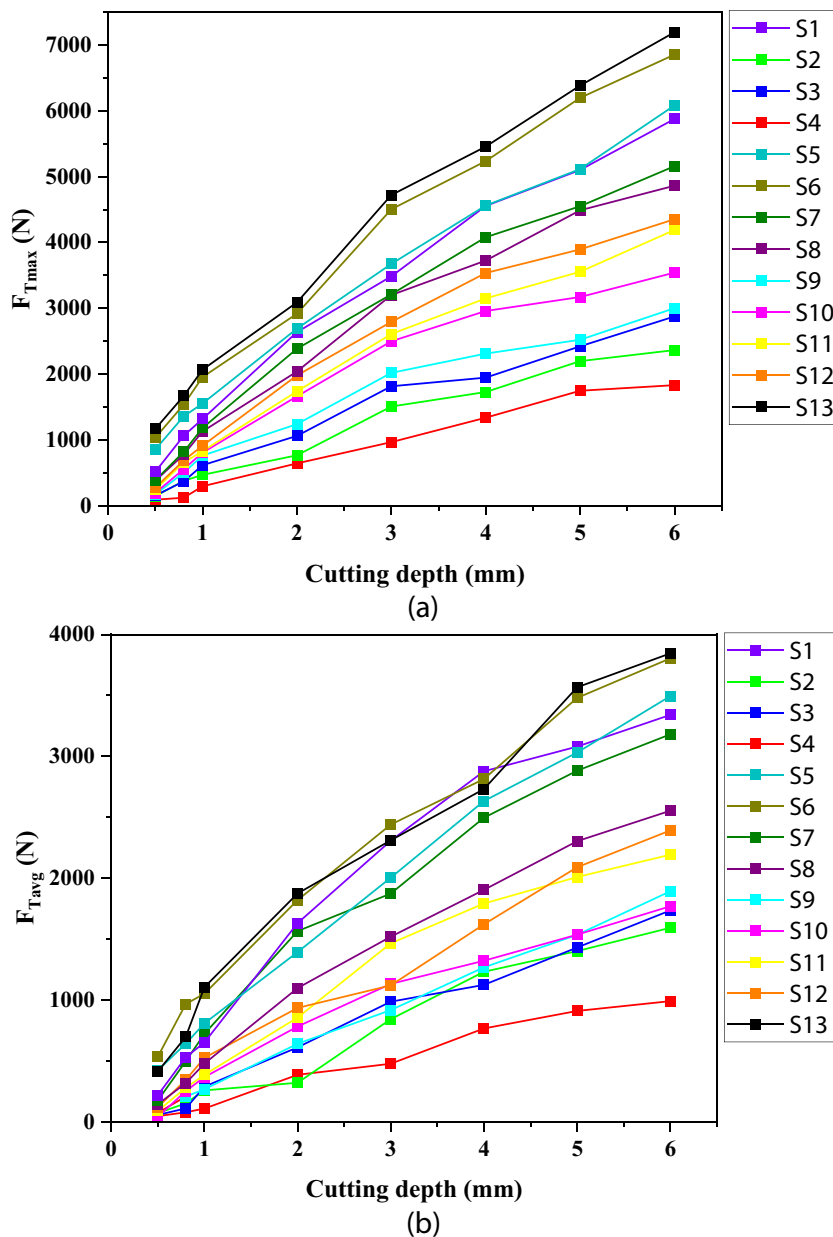
force increases, until the strength of the rock is exceeded. If the induced stresses by the tool exceeds the strength of the rock, it will result in extension of cracks, and suddenly the accumulated energy will be released. This release can be observed as a drop in the cutting force signal in the time domain. It is obvious that the larger the drop in forces, the larger the piece of rock created. Several scholars have deduced that these values can be connected with the failure modes of rocks (Che et al. 2014; Dai et al. 2021). Therefore, based on the cutting force at different cutting depths, the critical cutting depth (the depth beyond which the chip becomes visible) can be determined.

Dai et al. (2021) stated that through analysis of the ΔF- $\Delta F/\Delta T$ (ΔF-Ra) plot, it is possible to identify three regions: brittle, transition, and ductile, in rock cutting behaviour. Rock failure behavior, as determined by this plot, is characterized by the slope of the linear fit (SLR). In the ductile region, the SLR exhibits a smaller value close to zero, which then increases proportionally with brittle fracture, transitioning into the "transition" region. Eventually, the effect of ductile failure diminishes, and enters the brittle region. Figure 6 shows the ΔF-Ra plot of the cutting process, alongside the linear fit for sample S4 at a cutting depth of 2 mm. As can be seen, the region with a constant slope indicates that the cutting force increase with time remained steady. Due to the relatively stable process of rock cutting in this region, it indicates a ductile failure in the process. Figure 7 shows
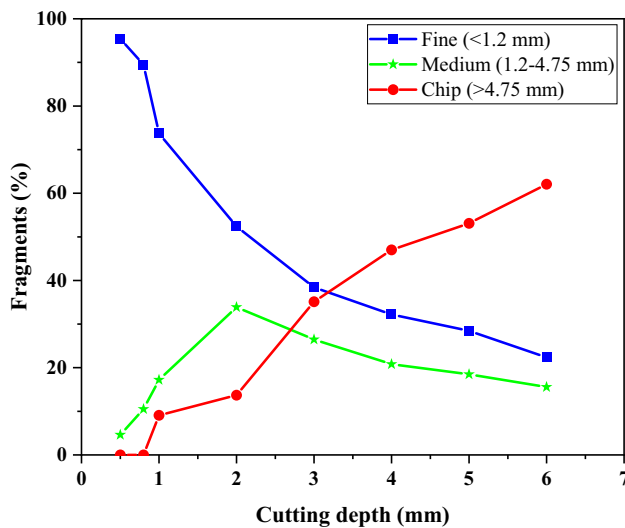
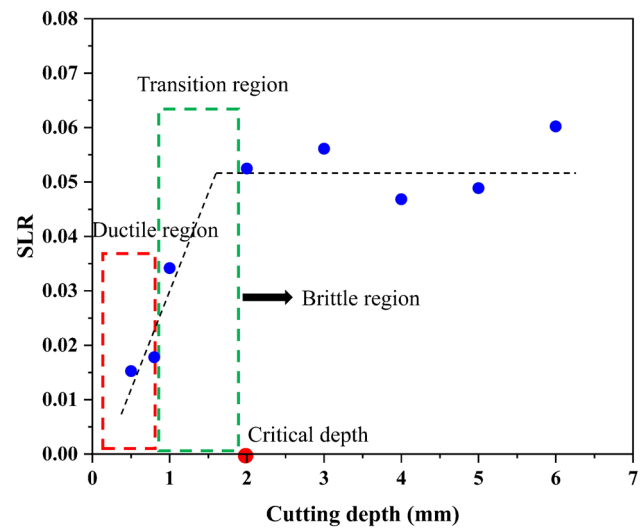**Fig. 5** The classification of fragments obtained from cutting the S9 rock sample

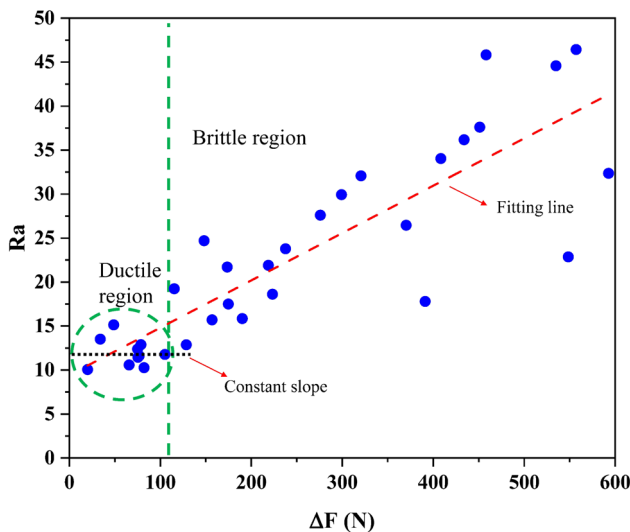**Fig. 7** The variations in SLR in relation to the depth of cut in sample S4

beyond 2 mm. Table 2 shows the critical cutting depth for rock samples.
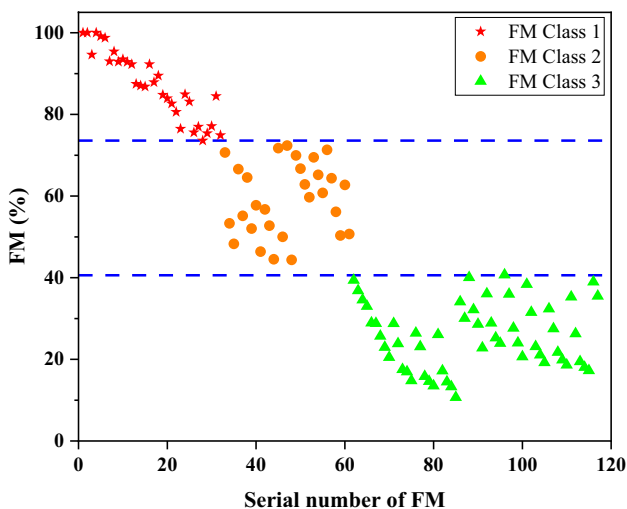
FM classification

In this section, the Hierarchical Clustering (HC) algorithm is used for FM classification relative to cutting geometry. This method is an unsupervised learning approach that groups data into a hierarchy or tree of clusters. This grouping is created based on the similarity or dissimilarity between the data in such a way that each cluster contains the most similar data and the least similarity exists between different clusters. In the hierarchical clustering method, a distance criterion (such as the Euclidean distance, Manhattan distance, Minkowski distance, and Chebyshev distance) is employed to measure the degree of similarity between the data points (Zhao and Karypis 2005). The distances can be expressed as a unified Minkowski distance according to Eq. 1 when tracking the variability of a parameter in 2D but in this study, a one dimensional measurement will suffice. The Minkowski distance is typically utilized with p-values of 1 or 2, corresponding to the Manhattan distance and the Euclidean distance, respectively. The Chebyshev distance, on the other hand, employs a value of p equal to infinity (Ketchen and Shook 1996).

$$d_{ij} = \sqrt{\sum_{a=1}^{p} (X_{ia} - X_{ja})^2} \qquad (1)$$

In this equation, X_{ia} and X_{ja} are the ath evaluation index of the fine material i and the fine material j, respectively, d_{ij} is the distance between the fine material i and the fine material

Fig. 6 The ΔF- ΔF/ΔT plot of the cutting process for sample S4 at a cutting depth of 2 mm

the variations in SLR as a function of the depth of cut in sample S4. According to this figure, for cutting depths of 0.5 mm and 0.8 mm, the slope changes were constant and lower compared to other depths. Consequently, sample S4 exhibited a ductile mode in these two cutting depths. As the cutting depth increased to 2 mm, the SLR also increased, and its value remained constant from a cutting depth of 2 mm onwards. Hence, the critical cutting depth for sample S4 is 2 mm. In other words, chips were observed at a cutting depth of > 2 mm for this sample, and the ratio of CH to FM increased as the depth increased

Table 2 The critical cutting depth of rock the samples

Sample	S1	S2	S3	S4	S5	S6	S7	S8	S9	S10	S11	S12	S13
Critical cutting depth (mm)	0.8	1	1	2	0.5	0.5	0.8	0.8	0.8	0.8	0.8	0.8	0.5

Fig. 8 FM classification after implementing HC algorithm

j, and P is the number of evaluator indicators from each FM class. In this paper, the value of P is equal to 1. In other words, "distance" is the difference between two FM values.

Finally, the clusters created based on a criterion called the linking criterion are connected to each other. There are various linking criteria, including single link, complete link, and the Ward criterion for linking clusters, among which the Ward criterion is more widely used (Eq. 2) (Johnson 1967). The Ward criterion is a method for determining how to merge clusters at each stage of the hierarchical clustering process. It is a cumulative approach, which means it begins with individual data points as separate clusters and then iteratively combines clusters that result in the smallest increase within-cluster sum of squares (Randriamihamison et al. 2021).

$$S = \sum_{t=1}^{k} \sum_{i=1}^{n_t} (X_i^{(t)} - \overline{X^{(t)}})'(X_i^{(t)} - \overline{X^{(t)}}) \qquad (2)$$

In this equation, n_t is the number of FM parameters in the G_t or group set (G_t is the set into which FMs are divided), $\overline{X^{(t)}}$ is the average value of the FM evaluator index in the G_t set, and S is the sum of the squared

deviations of the FM class. When S is minimized, it means that the set is chosen correctly.

The SPSS statistical software was utilized for FM classification based on HC algorithm. After applying the HC algorithm, new boundaries for the FM were determined as shown in Fig. 8. According to this figure, the FM class is divided into three categories: class 1 (FM percentage greater than 73.6%), class 2 (FM percentage between 73.6% and 40.6%), and class 3 (FM percentage less than 40.6%). Table 3 shows the conditions of FM production after classification. Various researchers have examined the cutting process and the creation of fragments, with a focus on both the brittle and ductile behavior regions (Richard et al. 2012; Zhou and Lin 2013; Jaime et al. 2015; Liu et al. 2018; Liu and Zhu 2019; Dai et al. 2021; Rostamsowlat et al. 2022). In contrast, some studies have focused on the behavior of the forces acting on the cutting tool within the brittle and ductile regions. However, the changes in cutting behavior and the classification of fines production based on these areas have not been discussed.

With the classification and critical cutting depth determined, it is now possible to analyze the production of FM and CH. For instance, based on the FM classification and critical cutting depth, Fig. 5 can be modified as depicted in Fig. 9. According to the figure, the critical cutting depth of the S9 sample is 0.8 mm. This depth signifies that if the cutting depth in this sample exceeds 0.8 mm, the failure mode is brittle, and the cutting operation is accompanied by chips. As shown in Fig. 9, after the depth of 0.8 mm, CH (rock pieces with dimensions larger than 4.75 mm) are formed. Furthermore, based on the FM classification, cutting depths less than 0.8 mm result in high FM production (indicating the presence of ductile failure mode). From a cutting depth of 1 mm to 3 mm, the percentage of FM production is considered medium, and for cutting depths exceeding 3 mm, the percentage of FM production is low. Hence, it can be deduced that fines production in the ductile failure mode is classified under class 1.

Transition zone

To establish a space that can determine the transition zone between the three FM regions based on the cutting operating conditions including F_{Tavg} and cutting rate (CR), the support

Table 3 The conditions of FM production after classification

FM condition	Class code	Representative color	FM percentage
High	1	■■■	>73.6%
Moderate	2	■■■	40.6-73.6 %
Low	3	■■■	<40.6%

Fig. 9 The S9 sample FM and CH production based on FM classification and critical cutting depth
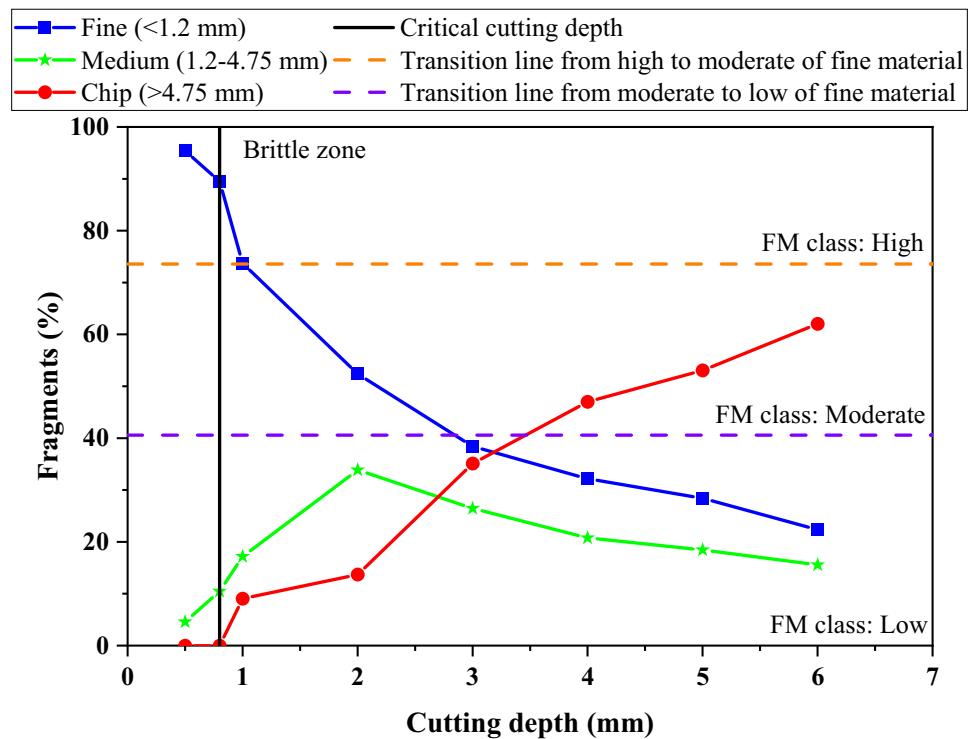
vector machine (SVM) algorithm is employed. SVM was initially developed to solve classification problems where the main goal is to find an optimal hyperplane that separates two classes. However, in reality, most problems involve multiple categories, which makes the traditional two-class support vector classification (SVC) unsuitable for multi-classification problems. To overcome this limitation, multi-class SVC conversion to multiple two-class SVCs was utilized. This approach categorizes multi-class methods into two groups: one-against-one (OAO) and one-against-all (OAA) algorithms (Ma and Guo 2014). The SVM algorithm transforms the initial training data into a higher dimension with the help of non-linear mapping. In this new dimension, it looks for an optimal hyperplane that linearly separates samples of one class from other classes. With a suitable non-linear mapping to a high enough dimension, the data of two classes can always be separated with the help of a hyperplane (Han et al. 2011). Indeed, the hyperplane serves as the boundary that separates two classes, transitioning into a line within two-dimensional space and into a plane within higher-dimensional spaces.

To develop SVM and determine the hyperplane (separating boundaries) for class separation and transition zone identification, coding in the MATLAB software environment has been used. The code begins by inputting the parameters (F_{Tavg} and CR). Next, the SVM algorithm was implemented using a tenfold cross-validation and a polynomial kernel function. Figure 10 shows the FM transition zone model based on SVM classification along with the decision boundaries. According to the graph, the two-dimensional space is divided into three

zones: high FM, moderate FM, and low FM, achieved through the use of two decision curves. Subsequently, based on the specified boundaries, the conditions of cutting depth during the excavation operation can be controlled in a manner that ensures it minimizes the excessive fines creation. It is important to mention that changes in the cutting depth directly impact two parameters: F_{Tavg} and CR. An excessive increase in cutting depth increases the force acting on the conical tool, leading to heightened machine vibrations, conical tool failure, and excavation machine damage. Therefore, cutting depth should also be regarded as a limiting factor to avoid excessive forces on the cutting tool or the machine.

Some of the previous studies have investigated the process of fines and chips production, considering the significance of the issue and its impact on cutting performance (Snowdon et al. 1982; Bruland 1998; Gertsch et al. 2007; Yin et al. 2014; Villeneuve 2017). Their findings align with those presented in this section. However, within this section, a framework has been developed to ascertain the fines zone using operational parameters. This framework enables the management of fines production to enhance productivity.

Performance of the transition zone

In order to assess the SVM model, four evaluation criteria including sensitivity (SE), accuracy (AC), specificity (SP), and Matthew's correlation coefficient (MCC) have been used. These criteria are determined using Eqs. 3, 4, 5, 6 based on the confusion matrix of the FM transition zone model (Ghasemi

Fig. 10 The developed FM transition zone model along with the decision boundaries
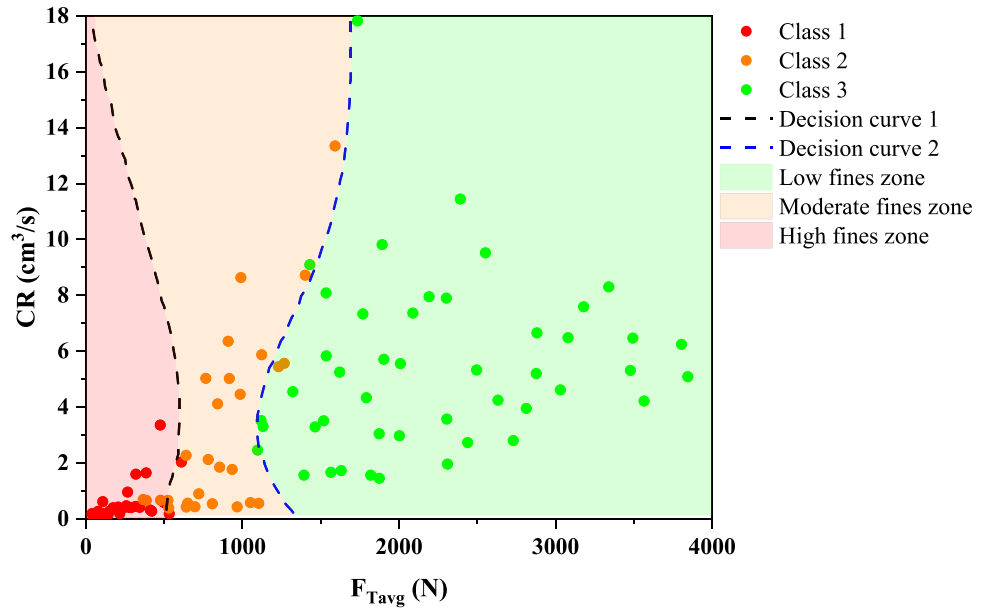
and Gholizadeh 2018; Kadkhodaei and Ghasemi 2022). Figure 11 shows the confusion matrix of SVM developed model.
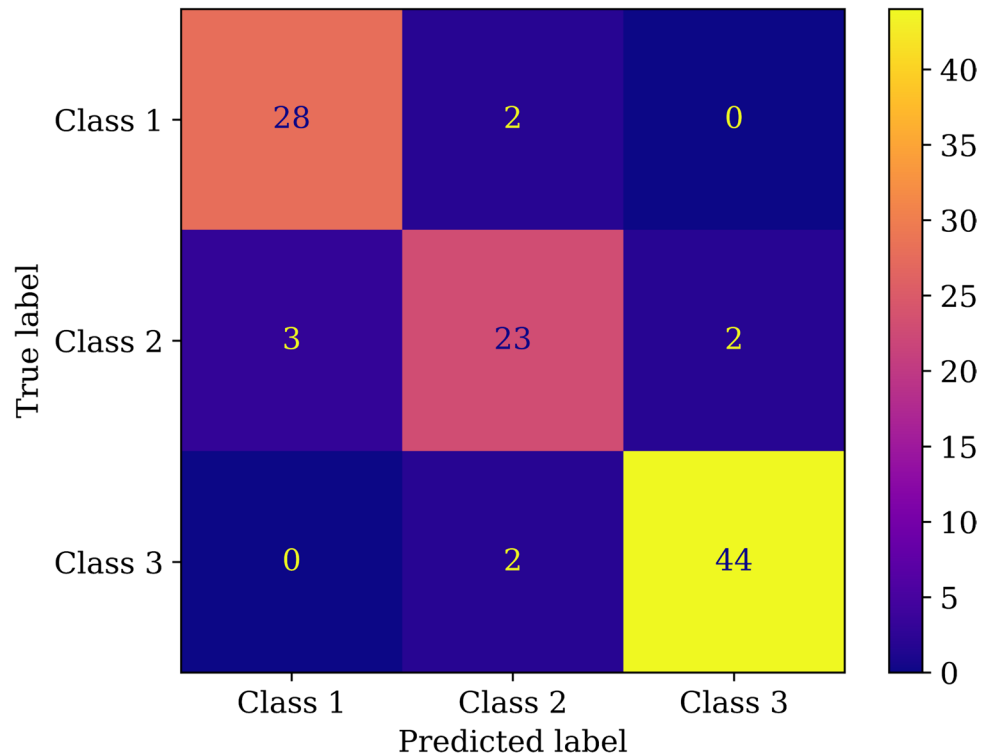
$$AC = \frac{TP + TN}{TP + TN + FP + FN} \tag{3}$$

$$SE = \frac{TP}{FN + TP} \tag{4}$$

$$SP = \frac{TN}{TN + FP} \tag{5}$$

$$MCC = \frac{(TP \times TN) - (FP \times FN)}{\sqrt{(TP + FN) \times (FP + TP) \times (FP + TN) \times (TN + FN)}} \tag{6}$$

where TP (true positive) is an outcome where the model correctly predicts the positive class, FP (false positive) is an

Fig. 11 The confusion matrix of FM transition zone model

outcome where the model incorrectly predicts the positive class, TN (true negative) is an outcome where the model correctly predicts the negative class and FN (false negative) is an outcome where the model incorrectly predicts the negative class.

AC, SE, and SP range from 0 to 1, with higher values indicating a more excellent model. On the other hand, MCC ranges between -1 and +1, where +1 represents a perfect prediction, 0 indicates no better than random prediction, and -1 signifies total disagreement between predicted and observed values (Kadkhodaei and Ghasemi 2022). Table 4 shows the values of SE, AC, SP and MCC for FM transition zone model. Based on the obtained results, the developed model has demonstrated high performance and can be effectively utilized to determine the transition zone of FM.

### Predicting the threshold cutting depth for efficient cutting

As mentioned, with the increase in cutting depth, the ratio of CH to FM also increases, and concurrently, it leads to an increase in F_{Tavg} and CR. However, increasing the cutting depth is also a limiting factor and cannot be raised to very high values due to the physical limitation of the cutting tool and negative effects on excavation operations. Therefore,

Table 4 Values of performance evaluation criteria for FM transition zone model

FM transition zone model	Class	AC	SE	SP	MCC
	1	0.952	0.933	0.959	0.884
	2	0.913	0.821	0.947	0.777
	3	0.961	0.956	0.965	0.922
	Overall	0.913	0.903	0.957	0.861

an effective limit should be determined based on the cutting depth in the FM transition zone. To determine the effective cutting depth, one can employ specific energy variations in relation to the cutting depth. Bilgin et al. (2006) noted that as the cutting depth increases (in unrelieved cutting mode), the specific energy decreases until the ratio of specific energy changes remains nearly constant when the cutting depth increases excessively (Fig. 12a). For this study, the effective cutting depth is determined by considering variations in specific energy of less than 10%. In other words, it is the depth at which the specific energy variations become less than 10%. Figure 12b shows the relationship between cutting depth and specific energy in the S4 rock sample with a threshold of 10%. According to this figure, the effective cutting depth for the S4 rock sample is 3 mm, where the specific energy variations are less than 10%. Table 5 shows the effective cutting depth and the corresponding values of each parameter. The effective cutting depth in this context corresponds to the minimum cutting depth where specific energy is minimized and its variations remain in specific energy nearly constant. This value is then utilized as minimum effective cutting depth (d_{Min}) in subsequent discussions.

To enhance comprehension of the effective conditions, Fig. 13 shows the relationship between F_{Tavg}, UCS, and FM within these conditions. It is important to highlight that F_{Tavg} values are normalized by using d_{Min}. As shown in the figure, there is a direct correlation between UCS and F_{Tavg}/d_{Min}; an increase in UCS leads to a rise in F_{Tavg}/d_{Min}. Furthermore, as F_{Tavg}/d_{Min} increases, there is a subsequent decrease in FM. This range delineates the conditions associated with the minimum cutting depth, while the range below it signifies the effective conditions for the cutting operation. Within this range, both the specific energy and subsequently the FM reach their minimum levels.
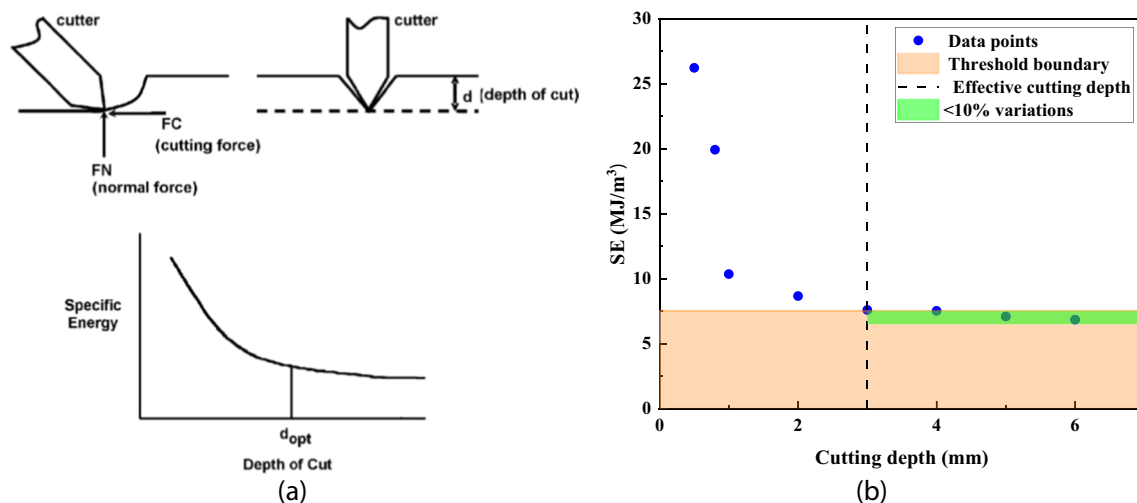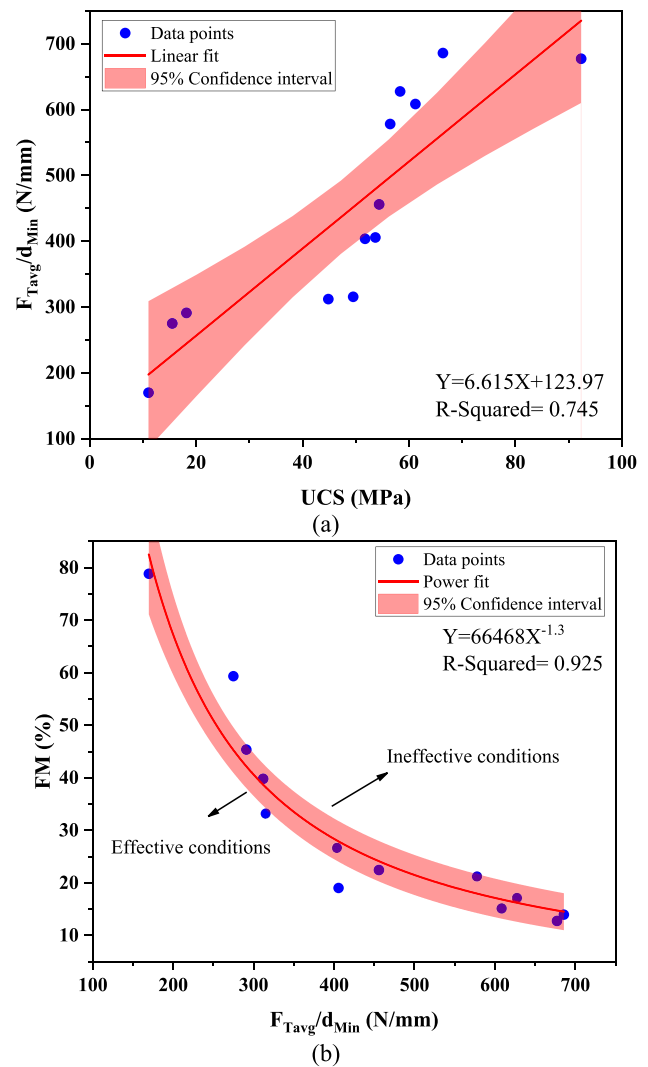

Fig. 12 The relationship between cutting depth and specific energy: **a**) Bilgin et al. (2006) and **b**) S4 rock sample with a threshold of 10%

Table 5 The effective cutting depth and the corresponding values of each parameter

Sample	Effective condition			
	d_{Min} (mm)	F_{Tavg} (N)	CR (cm^3/s)	FM (%)
S1	4.9	3074.29	6.45	17.12
S2	4.6	1267.60	7.78	59.34
S3	4.5	1321.37	8.98	45.37
S4	3.0	509.29	4.06	78.84
S5	5.2	3169.53	6.18	15.13
S6	4.8	3285.12	4.87	13.95
S7	4.5	2583.27	5.82	21.19
S8	4.6	2110.68	6.97	22.44
S9	4.3	1347.25	7.00	39.80
S10	4.8	1507.46	5.56	33.16
S11	4.5	1839.89	5.45	26.67
S12	4.8	1951.16	7.45	19.02
S13	5.7	3826.37	4.93	12.74

By incorporating the data points representing the minimum effective cutting conditions into Fig. 10, along with additional data concerning cutting depths greater than d_{Min}, a new operational zoning can be developed as shown in Fig. 14. According to this figure, the transition zone model is divided into five distinct ranges, including the minimum effective cutting depth limit, F_{Tavg} limit, CR limit, cutting tool geometry limit, and minimum allowable cutting depth limit. The minimum effective cutting depth limit indicates that when the cutting depth is chosen so that the values of F_{Tavg} and CR fall within Region 1, the conditions are deemed ineffective, resulting in an increase in FM and specific energy. The minimum allowable cutting depth limit indicates that performing cutting operations is inefficient when placed in Region 2 due to its location in a high fines zone. Due to limitations in cutting force applicable on the tool, there are other boundaries such as the F_{Tavg} limit, CR limit, and cutting tool geometry limit. Consequently, performing operations at high cutting depths (Region 3) is not feasible and it often leads to frequent tool failures. Based on these findings, by considering the two operating parameters F_{Tavg} and CR during rock cutting, it is possible to control fines production. Thus, the cutting depth is adjusted during the cutting process based on the applied forces and cutting rate, ensuring that the results remain within acceptable boundaries and the effective operating conditions are achieved. It is important to note that these results are preliminary and only relevant to the specific pick geometry discussed earlier in the paper, and should not be extrapolated to other types of picks or pick tip configurations.


Fig. 13 The relationship between F_{Tavg}, UCS, and FM at minimum effective cutting conditions

Future research directions

An overview of the literature reveals that there have been numerous comprehensive studies conducted on the impact of CH and FM production, as well as the dimensions of the fragments from cutting, on the performance of cutting. Nevertheless, a comprehensive investigation has yet to be conducted to ascertain the limit of FM production and develop effective rock cutting conditions. In this study, the SVM algorithm was utilized to investigate the boundary of FM production during rock cutting with a conical tool. This study represents the first attempt to manage fines production during cutting with a conical tool, and consequently, it has limitations that could enhance the comprehensiveness of the results by examining them in future studies:

Fig. 14 The FM transition zone and effective condition
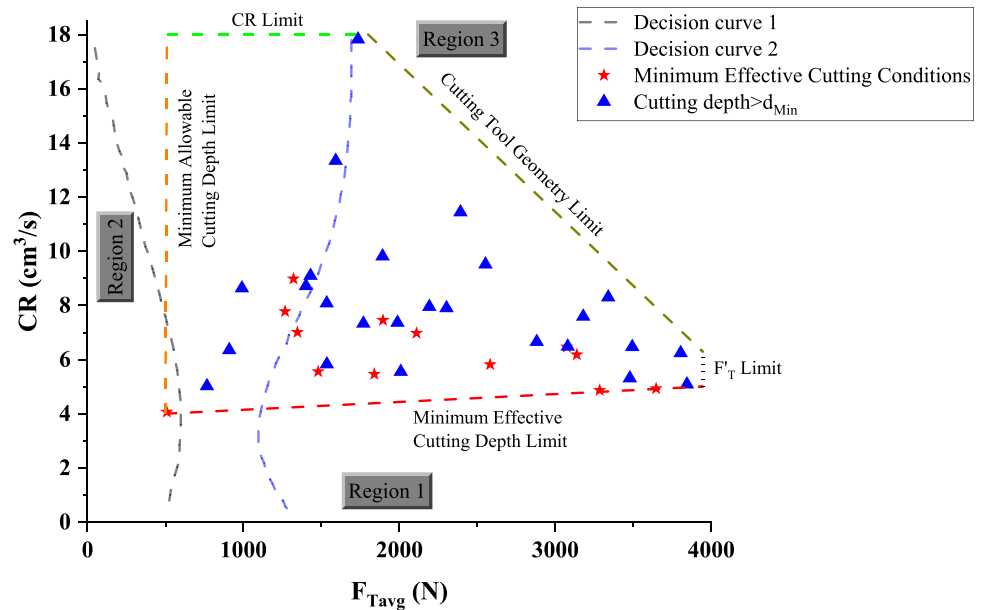
1) It should be noted that the analyses were developed based on controlled laboratory conditions in an unrelieved cutting mode, and considering other operational conditions, specially cut spacing, bit tip geometry, and attack angle may lead to generalizations of the analyses and results.

2) Examining and analyzing the results of additional rock samples, as well as investigating under special conditions such as the effect of water saturation and stress on the samples, can contribute to the usefulness of the study.

3) These results are preliminary and only relevant to the specific pick geometry discussed earlier in the paper, and should not be extrapolated to other types of picks or pick tip configurations. Furthermore, examining the relationship between the grooves in the relaxed cutting mode might aid in the completion of future investigations.

Summary and conclusions

In this study, the mechanism of fines and chip production was studied in rock cutting with a conical tool. Thirteen metamorphic and sedimentary rock samples with weak to medium strength values were carefully prepared and subjected to testing at different cutting depths: specifically, 0.5, 0.8, 1, 2, 3, 4, 5, and 6 mm. These measured forces allowed for analysis of cutting forces and specific energy while sampling of the cuttings facilitated assessment of the fines production. The threshold or critical cutting depth was determined by scrutinizing changes in the measured cutting forces with the goal of finding the transition zone between ductile

and brittle failure. The percentage of the fines was classified into three distinct classes using the hierarchical clustering algorithm. The results indicated that cutting depths below the critical cutting depth result in the generation of a significant amount of fines under the ductile failure mode.

Subsequently SVM algorithm was utilized to construct a two-dimensional space using cutting parameters (F_{Tavg}, and CR), facilitating the identification of the fines transition zone. The results derived from evaluating the performance of the two-dimensional fines space (utilizing AC, SE, SP, and MCC criteria) based on F_{Tavg}, and CR illustrated that the developed model proficiently assesses the fines transition zone with a high degree of effectiveness. The minimum effective cutting depth, at which the specific energy variations remained below 10%, was determined for each rock sample. Given that cutting performance parameters (F_{Tavg} and CR, FM) are a function of the cutting depth and the rock properties, some models are proposed for estimation of minimum penetration or cutting depth to ensure that the operation remains within the effective zone, minimizing the generation of excessive fines, excessive specific energy consumption, excessive machine vibrations, and associated damage.

Data Availability All data supporting the findings of this study are available within the paper.

Declarations

Competing interests The authors declare no competing interests.

References

Abu Bakar MZ, Gertsch LS (2011) Saturation efects on disc cutting of sandstone. In: Proceedings of the 45th US rock mechanics/geomechanics symposium. San Francisco, USA, pp 1–9

Abu Bakar MZ, Gertsch LS, Rostami J (2014) Evaluation of fragments from disc cutting of dry and saturated sandstone. Rock Mech Rock Eng 47:1891–1903. https://doi.org/10.1007/S00603-013-0482-8/FIGURES/17

Altindag R (2003) Estimation of penetration rate in percussive drilling by means of coarseness index and mean particle size. Rock Mech Rock Eng 36:323–332. https://doi.org/10.1007/S00603-003-0002-3

Altindag R (2004) Evaluation of drill cuttings in prediction of penetration rate by using coarseness index and mean particle size in percussive drilling. Geotech Geol Eng 22:417–425. https://doi.org/10.1023/B:GEGE.0000025043.92979.48

ASTM D2938-95 (1995) Standard test method for unconfned compressive strength of intact rock core specimens. American Society for Testing and Materials, West Conshohocken

ASTM D3967-95 (1995) Standard test method for splitting tensile strength of intact rock core specimens. Annual Book of ASTM Standards, American Society for Testing and Materials, West Conshohocken

ASTM D4543-08 (2008) Standard practices for preparing rock core as cylindrical test specimens and verifying conformance to dimensional and shape tolerances. Annual Book of ASTM Standards, American Society for Testing and Materials, West Conshohocken

Balci C (2009) Correlation of rock cutting tests with field performance of a TBM in a highly fractured rock formation: a case study in Kozyatagi-Kadikoy metro tunnel, Turkey. Tunn Undergr Space Technol 24:423–435. https://doi.org/10.1016/J.TUST.2008.12.001

Barker JS (1964) A laboratory investigation of rock cutting using large picks. Int J Rock Mech Min Sci Geomech Abstr 1:519–534. https://doi.org/10.1016/0148-9062(64)90059-2

Bejari H, Hamidi JK (2023) An experimental study of water saturation effect on chipping efficiency of a chisel pick in cutting some low- and medium-strength rocks. Rock Mech Rock Eng 1–27. https://doi.org/10.1007/S00603-023-03267-6

Bieniawski ZT (1989) Engineering rock mass classification. Wiley, New York

Bilgin N (1977) Investigation into mechanical cutting characteristics of some medium and high strength rocks. PhD Thesis, University of Newcastle upon Tyne, UK

Bilgin N, Copur H, Balci C (2014) Mechanical excavation in mining and civil industries. CRC Press, Taylor and Francis Group, London

Bilgin N, Demircin MA, Copur H et al (2006) Dominant rock properties affecting the performance of conical picks and the comparison of some experimental and theoretical results. Int J Rock Mech Min Sci 43:139–156

Bruland A (2000) Hard rock tunnel boring: vol 1–10. Norwegian University of Science and Technology (NTNU), Trondheim, Norway

Bruland A (1998) Hard rock tunnel boring design and construction. Norwegian University of Science and Technology, Trondheim, Norway

Che D, Han P, Peng B, Ehmann KF (2014) Finite Element Study on Chip Formation and Force Response in Two- Dimensional Orthogonal Cutting of Rock. Paper presented at the ASME 2014 International Manufacturing Science and Engineering Conference, Detroit, Michigan, USA. https://doi.org/10.1115/MSEC2014-3952

Copur H, Bilgin N, Tuncdemir H, Balci C (2003) A set of indices based on indentation tests for assessment of rock cutting performance and rock properties. J S Afr Inst Min Metall 103:589–599

Dai X, Huang Z, Shi H et al (2021) Cutting force as an index to identify the ductile-brittle failure modes in rock cutting. Int J Rock Mech Min Sci 146:104834. https://doi.org/10.1016/J.IJRMMS.2021.104834

Elbaz K, Shen SL, Zhou A et al (2021) Prediction of disc cutter life during shield tunneling with AI via the incorporation of a genetic algorithm into a GMDH-type neural network. Engineering 7:238–251. https://doi.org/10.1016/J.ENG.2020.02.016

Evans I, Pomeroy C (1966) The strength, fracture and workability of coal. Pergamon Press, Oxford

Gertsch L, Fjeld A, Nilsen B, Gertsch R (2000) Use of TBM muck as construction material. Tunn Undergr Space Technol 15:379–402. https://doi.org/10.1016/S0886-7798(01)00007-4

Gertsch R, Gertsch L, Rostami J (2007) Disc cutting tests in Colorado Red Granite: implications for TBM performance prediction. Int J Rock Mech Min Sci 44:238–246. https://doi.org/10.1016/J.IJRMMS.2006.07.007

Ghasemi E, Gholizadeh H (2018) Development of two empirical correlations for tunnel squeezing prediction using binary logistic regression and linear discriminant analysis. Geotech Geol Eng 2018 37:4 37:3435–3446. https://doi.org/10.1007/S10706-018-00758-0

Gong QM, Zhao J, Jiang YS (2007) In situ TBM penetration tests and rock mass boreability analysis in hard rock tunnels. Tunn Undergr Space Technol 22:303–316. https://doi.org/10.1016/J.TUST.2006.07.003

Han J, Pei J, Kamber M (2011) Data mining: concepts and techniques, 3rd edn. Morgan Kaufmann, San Mateo, CA, USA

Heydari S, KhademiHamidi J, Monjezi M, Eftekhari A (2019) An investigation of the relationship between muck geometry, TBM performance, and operational parameters: a case study in Golab II water transfer tunnel. Tunn Undergr Space Technol 88:73–86. https://doi.org/10.1016/J.TUST.2018.11.043

Hood M, Alehossein H (2000) A development in rock cutting technology. Int J Rock Mech Min Sci 37:297–305. https://doi.org/10.1016/S1365-1609(99)00107-0

Hou H, Liu Z, Zhu H et al (2021) An experimental study of the relationship between cutting efficiency and cuttings size in rock cutting using a PDC cutter. J Braz Soc Mech Sci Eng 43:1–12. https://doi.org/10.1007/S40430-021-02984-9

Huang D, Wang X, Su O et al (2022) Study on the cuttability characteristics of granites under conical picks by indentation tests. Bull Eng Geol Environ 81. https://doi.org/10.1007/s10064-022-02703-1

Ip C (1986) Laboratory water jet assisted drag tool rock cutting studies at high traverse speeds. University of Newcastle upon Tyne, UK

Jaime MC, Zhou Y, Lin JS, Gamwo IK (2015) Finite element modeling of rock cutting and its fragmentation process. Int J Rock Mech Min Sci 80:137–146. https://doi.org/10.1016/J.IJRMMS.2015.09.004

Jeong H, Jeon S (2018) Characteristic of size distribution of rock chip produced by rock cutting with a pick cutter. Geomech Eng 15:811–822

Johnson SC (1967) Hierarchical clustering schemes. Psychometrika 32:241–254. https://doi.org/10.1007/BF02289588

Kadkhodaei MH, Ghasemi E (2022) Development of a semi-quantitative framework to assess rockburst risk using risk matrix and

logistic model tree. Geotech Geol Eng 2022 40:7 40:3669–3685. https://doi.org/10.1007/S10706-022-02122-9

Ketchen D, Shook C (1996) The application of cluster analysis in strategic management research: an analysis and critique. Strateg Manag J 17:441–458

Liu W, Zhu X (2019) Experimental study of the force response and chip formation in rock cutting. Arab J Geosci 12:1–12. https://doi.org/10.1007/S12517-019-4585-8

Liu W, Zhu X, Jing J (2018) The analysis of ductile-brittle failure mode transition in rock cutting. J Petrol Sci Eng 163:311–319. https://doi.org/10.1016/J.PETROL.2017.12.067

Ma Y, Guo G (2014) Support vector machines applications. Springer International Publishing, New York

Martin JA, Fowell RJ (1997) Factors governing the onset of severe drag tool wear in rock cutting. Int J Rock Mech Min Sci 34:59–69. https://doi.org/10.1016/S1365-1609(97)80033-0

Mohammadi M, KhademiHamidi J, Rostami J, Goshtasbi K (2020) A closer look into chip shape/size and efficiency of rock cutting with a simple chisel pick: a laboratory scale investigation. Rock Mech Rock Eng 53:1375–1392

Morshedlou A, Rostami J, Moradian O (2023) Introducing a new model for prediction of mean cutting forces acting on conical pick cutters. Rock Mech Rock Eng 1–22. https://doi.org/10.1007/S00603-023-03636-1/FIGURES/15

Nishimatsu Y (1972) The mechanics of rock cutting. Int J Rock Mech Min Sci Geomech Abstr 9:261–270. https://doi.org/10.1016/0148-9062(72)90027-7

Pan Y, Liu Q, Liu J et al (2018) Full-scale linear cutting tests in Chongqing Sandstone to study the influence of confining stress on rock cutting efficiency by TBM disc cutter. Tunn Undergr Space Technol 80:197–210. https://doi.org/10.1016/J.TUST.2018.06.013

Pourhashemi SM, Ahangari K, Hassanpour J, Eftekhari SM (2021) Evaluating the influence of engineering geological parameters on TBM performance during grinding process in limestone strata. Bull Eng Geol Environ 80:3023–3040. https://doi.org/10.1007/S10064-021-02134-4

Randriamihamison N, Vialaneix N, Neuvial P (2021) Applicability and interpretability of ward's hierarchical agglomerative clustering with or without contiguity constraints. J Classif 38:363–389. https://doi.org/10.1007/S00357-020-09377-Y/FIGURES/11

Richard T, Dagrain F, Poyol E, Detournay E (2012) Rock strength determination from scratch tests. Eng Geol 147–148:91–100. https://doi.org/10.1016/J.ENGGEO.2012.07.011

Rispoli A, Ferrero AM, Cardu M, Farinetti A (2017) Determining the particle size of debris from a tunnel boring machine through photographic analysis and comparison between excavation performance and rock mass properties. Rock Mech Rock Eng 50:2805–2816. https://doi.org/10.1007/S00603-017-1256-5

Rostami J, Gertsch R, Gertsch L (2002) Rock fragmentation by disc cutter: a critical review and an update. In: Proceedings of the North American Rock Mechanics Symposium (NARMS), Tunneling Association of Canada (TAC) Meeting, Toronto, Canada

Rostami K, Hamidi JK, Nejati HR (2020) Use of rock microscale properties for introducing a cuttability index in rock cutting with a chisel pick. Arab J Geosci 13:1–12. https://doi.org/10.1007/S12517-020-05937-Z

Rostamsowlat I, Evans B, Sarout J et al (2022) Determination of internal friction angle of rocks using scratch test with a blunt PDC cutter. Rock Mech Rock Eng 2022 55:12 55:7859–7880. https://doi.org/10.1007/S00603-022-03037-W

Roxborough F (1973) Cutting rocks with picks. The Mining Eng, 445–455

Roxborough F, King P, Pedroncelli E (1981) Tests on the cutting performance of a continuous miner. J South Afr Inst Min Metall 81:9–25

Snowdon RA, Ryley MD, Temporal J (1982) A study of disc cutting in selected British rocks. Int J Rock Mech Min Sci Geomech Abstr 19:107–121. https://doi.org/10.1016/0148-9062(82)91151-2

Tuncdemir H, Bilgin N, Copur H, Balci C (2008) Control of rock cutting efficiency by muck size. Int J Rock Mech Min Sci 45:278–288. https://doi.org/10.1016/J.IJRMMS.2007.04.010

Villeneuve MC (2017) Hard rock tunnel boring machine penetration test as an indicator of chipping process efficiency. J Rock Mech Geotech Eng 9:611–622

Vogt D (2016) A review of rock cutting for underground mining: past, present, and future. J South Afr Inst Min Metall 116:1011–1026. https://doi.org/10.17159/2411-9717/2016/v116n11a3

Wang X, Su O, Wang Q feng (2022) Distribution characteristics of rock chips under relieved and unrelieved cutting conditions. Int J Rock Mech Min Sci 151:105048. https://doi.org/10.1016/J.IJRMMS.2022.105048

Wei Y, Yang Y, Tao M (2018) Effects of gravel content and particle size on abrasivity of sandy gravel mixtures. Eng Geol 243:26–35. https://doi.org/10.1016/J.ENGGEO.2018.06.009

Wei Y, Yang Y, Tao M et al (2023) Quantitative evaluation of service health condition for cutting tools on cutterhead in long-distance mechanized shield tunneling. Tunn Undergr Space Technol 137:105115. https://doi.org/10.1016/J.TUST.2023.105115

Wei YJ, Yang YY, Qiu T (2021) Effects of soil conditioning on tool wear for earth pressure balance shield tunneling in sandy gravel based on laboratory test. J Test Eval 49:2692–2706. https://doi.org/10.1520/JTE20180851

Wei YJ, Zheng X, Su F et al (2019) Evaluation of cutting tool wear of earth pressure balance shield in granular soil based on laboratory test. J Test Eval 47:927–941. https://doi.org/10.1520/JTE20180402

Wentworth CK (1922) A scale of grade and class terms for clastic sediments. J Geol 30:377–392. https://doi.org/10.1086/622910

Yin LJ, Gong QM, Zhao J (2014) Study on rock mass boreability by TBM penetration test under different in situ stress conditions. Tunn Undergr Space Technol 43:413–425. https://doi.org/10.1016/J.TUST.2014.06.002

Zhao Y, Karypis G (2005) Hierarchical clustering algorithms for document datasets. Data Min Knowl Disc 10:141–168. https://doi.org/10.1007/S10618-005-0361-3

Zhou Y, Lin JS (2013) On the critical failure mode transition depth for rock cutting. Int J Rock Mech Min Sci 62:131–137. https://doi.org/10.1016/J.IJRMMS.2013.05.004